HHS Public Access

Author manuscript

Nat Immunol. Author manuscript; available in PMC 2015 November 01.

Published in final edited form as:

Nat Immunol. 2015 May ; 16(5): 525–533. doi:10.1038/ni.3133.

Rapid Link of Innate Immune Signal to Adaptive Immunity by Brain–Fat Axis

Min Soo Kim[1,2,3], **Jingqi Yan**[1,2,3], **Wenhe Wu**[1,2,3], **Guo Zhang**[1,2,3], **Yalin Zhang**[1,2,3], and **Dongsheng Cai**[1,2,3]

[1]Department of Molecular Pharmacology, Albert Einstein College of Medicine, Bronx, NY 10461.

[2]Diabetes Research Center, Albert Einstein College of Medicine, Bronx, NY 10461.

[3]Institute of Aging, Albert Einstein College of Medicine, Bronx, NY 10461.

Abstract

Innate immunity signals induced by pathogen/damage-associated molecular patterns are essential for adaptive immune responses, but it is unclear if the brain plays a role in this process. Here we show that while tumor necrosis factor (TNF) quickly increased in the brain of mice following bacterial infection, intra-brain TNF delivery mimicked bacterial infection to rapidly increase peripheral lymphocytes, especially in the spleen and fat. Multiple mouse models revealed that hypothalamic responses to TNF were accountable for this increase of peripheral lymphocytes in response to bacterial infection. Finally, hypothalamic induction of lipolysis was found to mediate the brain's action in promoting this increase in peripheral adaptive immune response. Thus, the brain-fat axis is important for rapidly linking innate immunity to adaptive immunity.

Keywords

Innate immunity; adaptive immunity; brain; hypothalamus; TNF; lipolysis; fatty acid

Immune response is a vital mechanism for an organism to cope with harm and damage, a process which has innate immunity and adaptive immunity in vertebrates. Innate immune response represents a primary and immediate but rather non-selective defense through the actions of various innate immune molecules (e.g., tumor necrosis factor (TNF) and other cytokines) that are typically produced from innate immune cells such as macrophages[1-5]. In response to infections or tissue damage, innate immune cells are quickly activated by a

Correspondence should be addressed to D.C., Phone: 718-430-2426, Fax: 718-430-2433, dongsheng.cai@einstein.yu.edu.

AUTHOR CONTRIBUTIONS

D.C. conceived the hypothesis and designed the project and structures of experiments. M.S.K. co-designed, developed and performed all experiments as presented in this paper. J.Y. did viral injection, histology and immunostaining; W.W. contributed to animal generation, sample preparations and flow cytometry procedure; G.Z. co-designed and did preliminary experiments for Figure 1 and 7; Y.Z. did viral cloning and generated viruses. M.S.K. and D.C. performed data analysis, and all authors participated in discussion. D.C. wrote the paper, and M.S.K. prepared all figures and provided writing assistance.

COMPETING INTERESTS STATEMENT

The authors state that they have no competing financial interests.

group of lipid-based molecules known as pathogen-associated molecular patterns (PAMPs), which consist of lipopolysaccharide (LPS), peptidoglycan and lipoteichoic acids, or by damage-associated molecular patterns (DAMPs) that comprise a broader range of molecules released from stressed or damaged cells[1-5]. Differing from innate immunity, adaptive immunity is a specialized immune response that is mediated by T and B lymphocytes from immune organs, and it often requires a prolonged period (4 to 7 days) for these cells to become effector cells. Innate immunity signals are crucial for initiating adaptive immune responses[1-5], for instance, TNF and interleukins play a critical role in stimulating T and B cells[6]. While this connection between innate and adaptive immunity has been appreciated to be the case locally in peripheral immune organs, an intriguing question is whether this immune crosstalk requires a systemic regulation by such as the central nervous system (CNS). Herein, in the context of our research which focused on studying hypothalamic innate immune pathways[7-11], we explored if the brain is important for rapidly conveying innate immune signals to initiate adaptive immunity.

Results

Initiation of adaptive immunity by central TNF action

We employed an infection model in which wild-type C57BL/6 mice were injected with *Listeria monocytogenes*, a gram-positive bacterium that is a well-established pathogen to induce innate and adaptive immune responses[12,13]. We found that, in addition to its rise in the plasma, TNF concentrations in the cerebrospinal fluid (CSF) quickly increased in mice at day 1 after receiving an intravenous injection of *L. monocytogenes* (**Supplementary Fig. 1a**). Our immunostaining verified that TNF receptor 1 (TNFR1) is abundantly expressed in the mediobasal hypothalamus (MBH) (**Supplementary Fig. 1b**). We then asked if delivering TNF in the brain of mice had an effect on systemic immunity. To do so, we injected wild-type C57BL/6 in the hypothalamic third ventricle with TNF at a low dose (10 pg); following this injection, TNF concentrations in the CSF increased as similarly seen in *L. monocytogenes*-infected mice (**Supplementary Fig. 1c**). However, this injection dose did not affect blood concentrations of TNF (37.92 ± 3.94 vs. 38.23 ± 2.74 pg/ml in TNF- vs. vehicle-injected mice, $P = 0.48$). Because we were interested if brain responses have a rapid effect on immunity, we used a 3-day experimental course, which reflects an early time point in this immune response and also provides a necessary time window to induce cell proliferation. We confirmed that 3-day injections of low-dose TNF did not lead to sickness in mice, and therefore this pharmacological model is physiologically suitable for this study.

Using flow cytometry, we found that this hypothalamic low-dose TNF injection did not change the numbers of macrophages in the peripheral tissues or blood (**Supplementary Fig. 2a–c**). However, this hypothalamic TNF injection led to evident increases in T and B cells in the spleen as compared to vehicle injection, and these effects were associated with proportional increases in splenic $CD4^+$ and $CD8^+$ T cells in these mice (**Fig. 1a–e**). Notably, fold increases of $CD4^+$ and $CD8^+$ cell numbers were more remarkable in the epididymal fat of TNF-injected mice (**Fig. 1a,f–h**), compared to the spleen of these mice, and B cell numbers in the epididymal fat of these TNF-injected mice also clearly increased (**Fig. 1a,i**). The increase in lymphocytes in these TNF-injected mice were comparable to the increase of

these cells observed in mice following 3 days of bacterial infection (**Supplementary Fig. 2d–k**). We predicted that increased numbers of splenic and adipose lymphocytes in TNF-injected mice might lead to increased lymphocyte numbers in the circulation. Flow cytometry of the blood of these mice supported this prediction (**Fig. 1a, Supplementary Fig. 3a–d**). Other tissues of TNF-injected mice, such as liver, skeletal muscle, heart and kidney, were also subjected to flow cytometric analysis, but few lymphocytes were found in these tissues and did not change upon TNF injection.

To further demonstrate the immunological relevance of this finding, we profiled subsets of T and B cells after hypothalamic injections of TNF. First, flow cytometry was used to analyze $ICOS^+PD\text{-}1^+$ and $PD\text{-}L1^+$ cells, as these populations represent activated T and B lymphocytes. Increased numbers of $ICOS^+PD\text{-}1^+$ cells were observed in the epididymal fat and spleen as compared to vehicle control (**Supplementary Fig. 3e–h**), suggesting that T and B cells in these tissues were activated in response to hypothalamic TNF injection. BrdU staining revealed that TNF-injected mice showed strong cell proliferation in the spleen and epididymal fat, compared to vehicle-injected mice (**Fig. 1j**). Subsequently, we used flow cytometry to profile $CD4^+$ helper (T_H) cell subsets, including T_H1 ($CD4^+CXCR3^+$), T_H2 ($CD4^+CXCR3^-$) and T_H17 ($CD4^+CCR6^+$). Hypothalamic ventricular TNF injection increased or tended to increase each of these T_H subsets in the spleen and epididymal fat (**Supplementary Fig. 3i–n**). Regulatory $CD4^+$ T cells were analyzed using Foxp3 and CD25; however this hypothalamic TNF injection did not increase the numbers of $CD4^+Foxp3^+CD25^+$ cells in the spleen or fat (data not shown). In summary, brain TNF action has an effect in increasing and activating peripheral lymphocytes.

Adaptive immune initiation in infection via brain TNF action

To evaluate if the observed effects of TNF were brain-specific, we subjected C57BL/6 mice to peripheral injections (i.p.) of TNF, using the same low dose (10 pg) as we used in our hypothalamic injection experiments. Flow cytometric analysis confirmed that peripheral injection of low amounts of TNF did not change the numbers of $CD4^+$ and $CD8^+$ T or B cells in the spleen, epididymal fat or blood (data not shown). For comparison, we administrated TNF at a pathological, high dose (5 ng) in C57BL/6 through i.p. injection, which mimicked the increase of serum TNF under bacterial infection. TNF concentrations in the CSF of these TNF-injected mice increased ~3 fold, compared to the normal baseline concentrations in control mice. This high-dose TNF treatment over 3 days increased $CD4^+$ and $CD8^+$ T cells and B cells in the spleen and epididymal fat (data not shown). We thus hypothesized that infection-induced increase of circulating TNF leads to the observed effects of central TNF, given that the MBH vasculature is permeable[14], this permeability is enhanced under infection[15]. To test this idea, we studied if bacterial infection-induced adaptive immune responses could be altered by suppressing TNF signals in the brain. Therefore, we pre-injected C57BL/6 mice in the hypothalamic ventricle with TNF antagonist WP9QY one day prior to bacterial infection, and then maintained daily hypothalamic injections of WP9QY for 3 days before flow cytometric analysis. This WP9QY treatment substantially dampened the induction of adipose $CD4^+$ and $CD8^+$ T cells as well as B cells by infection (**Fig. 2a–e**). Also, these WP9QY-treated mice showed impaired increases of these lymphocytes in the spleen under bacterial infection (**Fig. 2a,f–i**).

Hence, all these data support the hypothesis that TNF signals in the brain contribute to initiation of adaptive immune responses.

Hypothalamic TNF action initiates adaptive immunity

Because the MBH, especially the comprised arcuate nucleus, strongly expresses TNFR1, we reasoned that the MBH is critical for the action of central TNF in increasing peripheral lymphocytes. To test this concept, we examined if blocking TNF receptors in the MBH was sufficient to affect adaptive immune response during *L. monocytogenes* infection. Using site-specific delivery of lentiviral shRNA as we established previously[16], we generated mice with MBH-directed TNF receptor knockdown. In this approach, we knocked down TNFR1 as well as TNFR2 to eliminate possible redundancy between these two isoforms. Expression of TNFR1 and TNFR2 protein in the MBH was reduced by shRNA knockdown (**Fig. 3a**). These mice and the scramble shRNA-injected control mice received an intravenous injection of *L. monocytogenes*; at 3 days post-infection, various tissues were collected and subjected to flow cytometry. We found that infection-induced increases in adipose $CD4^+$ T, $CD8^+$ T, and B cells were severely impaired in TNFR knockdown mice, compared to scramble shRNA group (**Fig. 3b–f)**. Knockdown of TNF receptors also significantly impaired the induction of splenic $CD4^+$ T, $CD8^+$ T and B cells by infection (**Fig. 3b,g–j**). In addition, we generated mice in which TNFR was inhibited in the pro-opiomelanocortin (Pomc) neurons in the MBH, and found that this manipulation reduced the effects of central TNF in increasing adipose $CD4^+$ T, $CD8^+$ T and B cells (**Supplementary Fig. 4a–d**). Thus, based on the collection of these results, the mediobasal region of the hypothalamus is important in linking brain TNF signal to adaptive immunity.

To further study the role of hypothalamic TNF in initiating adaptive immune responses, we employed a genetic mouse model that is deficient of TNFR1 and TNFR2[17,18]. We crossed TNFR1-deficient mice (*Tnfrsf1a*$^{-/-}$) with TNFR2-deficient mice (*Tnfrsf1b*$^{-/-}$), leading to doubly deficient homozygote (TNFR-null). TNFR-null mice are extremely vulnerable to bacterial infection[17,18]. We confirmed that adaptive immune responses to infection were severely impaired in these mice. In this context, we studied if the adaptive immunity impairment in TNFR-null mice could be reversed, perhaps partially, by restoring TNF receptor in the MBH. To do so, we injected lentiviral TNFR1 bilaterally in the MBH of these TNFR-null animals using MBH-directed injection[8,9,11,16]. TNFR-null mice injected with lentiviruses lacking TNFR1 were used to provide a viral control group. Using immunostaining, we verified that lentiviral expression of TNFR1 led to a restoration of TNFR1 protein in the MBH and especially the comprised arcuate nucleus of TNFR-null mice (**Fig. 4a**). Thus, we generated a mouse model in which TNF receptor was absent in the whole body except for the MBH, providing a unique tool to specifically dissect out the MBH-specific role of TNF receptors in immune response.

Using the animals described above, we challenged them with bacterial injection to induce adaptive immune responses. We compared bacteria-injected TNFR-null mice that received lentiviral delivery of TNFR1 vs. vector control in the MBH. The lentiviral vector control group of TNFR-null mice showed fewer splenic and adipose $CD4^+$ T, $CD8^+$ T and B cells (**Fig. 4b–j**), similar to that seen in TNFR-null mice that did not receive MBH injection (data

not shown). In contrast, the delivery of TNFR1 in the MBH completely or partially restored the increase in adipose lymphocyte numbers in TNFR-null mice in response to infection (**Fig. 4b–f**). Splenic T and B cell numbers in these mice also increased, although to lesser extents compared to fat tissues (**Fig. 4g–j**). As a measurement of immune function in combating infection, fewer viable bacteria were found in TNFR-null mice that received MBH injections of lentiviral TNFR1 as compared to the control lentiviral group (**Supplementary Fig. 4e–g**), indicating that TNFR1 restoration in the MBH can decrease the severity of infection in various tissues of the TNFR-null mice. Thus, TNF pathway in the hypothalamus is required for the induction of adaptive immunity against bacterial infection.

Lipolysis links the CNS to adaptive immune response

We subsequently asked what molecules could be responsible for the brain's action in mobilizing adaptive immune cells. To address this question, we measured the mRNA abundance of innate immunity cytokines such as interleukin-1β (IL-1β) and interleukin-6, and observed that hypothalamic injection of TNF did not change the mRNA abundance of these cytokines in the fat (data not shown), arguing against adipose innate immunity being a key mediator for the effect of central TNF on adaptive immunity. By contrast, such delivery of TNF increased the mRNA expression of lipolytic genes in the fat, including hormone-sensitive lipase (*Lipe*), lipoprotein lipase (*Lpl*), and acyl-CoA synthetase long-chain family member-1 (*Acsl1*) (**Fig. 5a**). Lipolysis is a characteristic for infection, and some fatty acids have recently been linked to immunity[19-23], but it remains unexplored if lipolysis is important for the brain–fat axis to initiate adaptive immune responses, despite that previous studies revealed a role for lipids in T cell development[24]. We directed our research attention to the brain–fat axis by asking if the brain might regulate lipolysis to aid adaptive immunity. Indeed, hypothalamic injection of TNF substantially increased fatty acids in the blood by eliciting concentrations that were ~2.6 times higher compared to the basal levels in vehicle-injected mice (**Fig. 5b**). In agreement, the blood concentrations of fatty acids in *L. monocytogenes*-infected mice were ~3 times higher than the levels in the control mice (**Fig. 5c**). This effect was consistent with increased expression of lipolysis genes in the fat of bacteria-infected mice (**Fig. 5d**). By analyzing fatty acid species, we found that central TNF injection or bacterial infection strikingly increased the serum concentrations of several long-chain fatty acids (**Supplementary Fig. 5a**). In agreement with these results, endotoxin-treated mice were reported to increase lipolysis and blood fatty acids[25]. Thus, we hypothesized that brain-induced lipid release might work as a link for the relationship among the brain, fat and adaptive immune cells.

To directly evaluate the potential role of fatty acids in adaptive immunity, we analyzed bacteria-infected mice in which brain TNF or hypothalamic TNF receptor function was inhibited. We found that bacteria-induced increases in blood fatty acids were attenuated in these mice when brain or hypothalamic TNF was inhibited pharmacologically (**Fig. 5e**) or genetically (**Fig. 5f**). We then examined if administration of a long-chain fatty acid species could lead to an increase in lymphocytes. Using the 3-day experimental duration, we injected C57BL/6 mice with either palmitic or linoleic acid at a suitable dose (5 mg/kg/day, i.p.). We found that palmitate treatment led to evident increases in adipose $CD4^+$ T, $CD8^+$ T cells and B cells (**Fig. 5g–j**). Palmitate also increased splenic lymphocyte numbers (**Fig. 5k–**

n); however, palmitate treatment in this dosage and duration did not clearly increase macrophage numbers in the fat or spleen (data not shown). Compared to palmitate, linoleic acid at this dose did not increase adipose lymphocyte numbers (**Fig. 5g–j**), but had an effect in increasing splenic lymphocytes (**Fig. 5k–n**). Oleic acid was also tested, but showing that its injection at the same dose did not increase lymphocyte numbers in the fat or spleen (data not shown). Thus, despite that the effects of individual fatty acid species on tissue lymphocytes were dynamic, these observations support the general idea that brain-induced lipolysis plays a role in linking the brain–fat axis to adaptive immune response.

Central TNF-induced lipolysis initiates adaptive immunity

Loss-of-function experiments were simultaneously developed to study if fatty acids could be inhibited to cause an impaired effect of brain TNF in stimulating adaptive immunity. In these experiments, we i.p. injected C57BL/6 mice with a fatty acid synthase inhibitor, cerulenin, at the dose of 10 mg/kg/day for 3 days before these mice received daily hypothalamic third-ventricle injections of TNF (10 pg). While lymphocyte numbers in the fat of these mice increased by the central injection of TNF, these changes in the fat were completely prevented by cerulenin pre-treatment (**Fig. 6a–d**). Notably the effects of central TNF in increasing splenic T and B cells were also abolished by cerulenin pre-treatment (**Fig. 6e–h**), suggesting that release of fatty acids from the fat has an effect in initiating the increase of splenic lymphocytes.

We asked if this lipid-based effect also applied to bacterial infection. To examine this possibility, we administrated that same dose of cerulenin (10 mg per kg body weight per day) to mice on the day before other treatments, followed by a single intravenous injection of *L. monocytogenes* or vehicle while daily intraperitoneal injections of cerulenin continued for 3 d. Flow cytometry revealed that cerulenin treatment reduced the magnitude of bacterial infection-induced increases of lymphocytes in the fat as well as the spleen (**Fig. 6i–p**). For comparison, we simultaneously analyzed macrophages in these tissues, showing that cerulenin treatment did not prevent bacteria from increasing these innate immune cells (data not shown). To gain a further insight into the brain–fat connection in adaptive immune response, we performed epididymal fat denervation to break the brain–fat axis. Indeed, sympathetic denervation in the white fat has been established as an approach to inhibit lipolysis[26-28]. We found that fat denervation reduced the effects of brain TNF in increasing adipose lymphocyte numbers (**Fig. 7a–e**). The effects of brain TNF in increasing splenic T and B cells were also reduced by fat denervation (**Fig. 7f–i**), suggesting that the epididymal fat is important in conveying the brain signal into the spleen. In summary, brain induction of lipid release is important for adaptive immunity in a manner that is independent of innate immunity.

Lypolysis requires leptin release to increase lymphocytes

The data presented above support the point that lipolysis is a vital mediator for the effects of the CNS in regulating adaptive immune cells. In this background, we reasoned that lipolysis requires other secretory factors from the fat in this regulation, which is likely since lipolysis *per se* can be induced in immunity-unrelated metabolic conditions such as starvation. We appreciated that infection-induced lipolysis is typically accompanied by increased release of

adipokines such as leptin. This characteristic differs from the features in starvation during which leptin release from the fat is in fact suppressed. Of note, systemic leptin has been shown to enhance the function of immune organs[46], and besides, acute increase of leptin has a strong metabolic effect in increasing lipolysis. We analyzed blood samples from several mouse models in this study, and found that serum leptin concentrations increased in animals in response to central TNF injection or bacterial infection, and TNFR in the MBH was required for this effect (**Supplementary Fig. 5b–e**). We then studied the potential relationship between fatty acid and leptin release in affecting adaptive immune response. Using cerulenin pre-treatment, we found that inhibition of lipolysis impaired leptin i.p. injection from increasing lymphocytes (**Supplementary Fig. 6a–h**), indicating that lipolysis mediates leptin-induced adaptive immune response. Interestingly, we also found that blocking systemic leptin through leptin neutralization led to compromised effects of palmitate in increasing T and B cells (**Supplementary Fig. 7a–h**), suggesting that the release of fatty acids and leptin from the fat cooperate with each other in inducing adaptive immune responses.

Chronic neuroinflammation impairs adaptive immune response

Previous studies have shown that the baseline levels of innate immunity signals are high in the hypothalamus under conditions of obesity and associated metabolic disorders[7-11]. Thus, we asked if chronic hypothalamic inflammation in this metabolic model might have an impact on the central regulation of adaptive immunity. To do so, we compared mice with diet-induced obesity versus chow-fed normal mice by subjecting these animals to the central injection of TNF, using the same dose and duration as described above. In agreement with the previous reports[29,30], we noted that compared to normal mice, lymphocyte numbers in the fat of obese mice were higher (**Fig. 8a–d**). However, in response to hypothalamic injection of low-dose TNF, adipose T and B cell numbers failed to increase, whether the calculations were based on cell numbers per fat pad (**Fig. 8a–d**) or per gram (data not shown) of epididymal fat. Splenic lymphocytes in these mice were also studied, showing that there was a lack of responsiveness to the hypothalamic injection of TNF in obese mice (**Fig. 8e–h**). To gain an insight into the underlying basis, we analyzed the hypothalamus for a list of TNF-induced inflammatory genes including *Nfkbia*, *Il1b*, *Il6* and *Socs3*. We found that under the basal condition, mRNA expression of these genes was generally elevated in the hypothalamus of obese mice compared to that seen in chow-fed normal mice (**Fig. 8i–l**). In response to a hypothalamic injection of TNF at the low-dose dose, the mRNA abundance of these genes in the hypothalamus substantially increased in normal mice but weakly or negligibly increased in obese mice (**Fig. 8i–l**). This reduction in hypothalamic responsiveness to TNF explains for the observed impairment of adaptive immunity in obesity, indicating that a responsive hypothalamic environment for innate immunity signals such as TNF is necessary for the brain to acutely regulate adaptive immune response.

Discussion

Based on *in vitro* and *in vivo* models, cytokines such as TNF are produced from innate immune cells like macrophages and play a critical role in conveying innate immunity to adaptive immunity[6]. However, as adaptive immune response typically requires 4 to 7 days

to develop, it is a major limitation for an organism to fight against an invasion which becomes overwhelming quickly after initial attack[4,5]. Therefore, to study the early process and regulation in adaptive immune response is important, and understanding of the underlying basis may help development of new strategies by which lymphocytes are promoted in a rapid fashion to aid adaptive immune response. Here, we discovered that the brain and, in particular the hypothalamus, quickly responds to innate immunity signal TNF and employs the brain–fat axis to initiate the increases of T and B cells in peripheral tissues including the fat and spleen. The brain is best known for its fast action in regulating physiology, but a possible relevance of this feature to immunology has not been much explored. Regardless, it has been shown that the brain can answer innate immune cytokines to alter the sympathetic nerve system activities, and TNF is a cytokine which can rapidly induce neural synaptic change in experimental autoimmune encephalomyelitis[31]. Also, as observed clinically and experimentally, brain injuries are often associated with immune impairments and high susceptibility to infection, and it was suggested that the hypothalamus is a factor which mediates systemic immune depression[32]. Interestingly, it was recently found that activation of certain neuronal pathways can downregulate peripheral innate immune responses[33-36], although the hypothalamus has not been studied in this context. Thus, in conjunction with our findings here, we suggest that the hypothalamus–periphery axis has an unappreciated role in regulating immune homeostasis by improving the sensitivity and efficiency of adaptive immunity on one hand and preventing against excess innate immune response on the other hand.

Previously, it has been revealed that the hypothalamus employs innate immunity pathways to exert metabolic changes[7-11], and hypothalamic actions from innate immune cytokines have strong effects on the metabolic state of fat[37,38]. Since the blood–brain barrier surrounding the MBH is partially permeable[14,15], this hypothalamic region represents a critical site for studying involvements of the brain–peripheral communications in physiology including systemic immunity[39]. In this work, we asked if the brain might work through a hypothalamus–fat axis to coordinate innate immunity signals with adaptive immunity. This question is provocative, because unlike innate immunity, the operation of adaptive immunity is orchestrated by specialized immune organs such as the spleen, while fat tissue is not classically viewed as a component in adaptive immunity. However, fat tissue has appreciable numbers of immune cells, including not only innate immune cells such as macrophages but adaptive immune cells including T and B cells[29,40,41]. While innate immune cells in the fat have often been related to the development of metabolic disorders such as type-2 diabetes[42,43], the biological function of adaptive immune cells in fat tissue is still unknown. Recently, it was reported that $CD8^+$ T cell memory function was enhanced by modulating fatty acid metabolism in mice[24], which might hint for a role of fat tissue via lipid metabolism in adaptive immunity. Here, we showed that the fat is an organ with a function to support the initiation of adaptive immunity, and the hypothalamus is responsible for ensuring this function. Indeed, it is well documented that severe lack of fat in the body, such as lipodystrophy, is extremely injurious for adaptive immunity[44]. Ironically, fat excess in diseases such as obesity is also detrimental for adaptive immunity, and we provided evidence suggesting that obesity-associated chronic neural inflammation blunts the hypothalamic regulation on adaptive immune response. Altogether, our findings indicate

that a homeostatic and responsive hypothalamus–fat axis is necessary for adaptive immunity. Moreover, since fat tissue is distributed throughout the body as widely as lymphoid tissue, our findings may lead to a viewpoint that components of adaptive immunity can be extended to include fat tissue.

In this work, we also initially investigated the route by which the brain–fat axis works to increase lymphocytes in the periphery. Our findings suggest that the hypothalamus employs the sympathetic nervous system to induce lipolysis and release of long-chain fatty acids and thus increase adipose and splenic lymphocytes. The sympathetic induction of lipolysis is rapid, which fits within the fast action of the brain–fat axis in promoting adaptive immune cells. Consistent with this finding, it has recently been reported that changes in fatty acid metabolism affects $CD8^+$ T cells[24], and palmitate was reported to increase proliferation of T lymphocytes[45]. In this context, we also considered that lipolysis *per se* can be induced in conditions (e.g., starvation) which may be unrelated to immunity. However, infection-induced lipolysis has several characteristics, for example, it is profoundly associated with release of adipokines such as leptin, which might exert cooperative actions with fatty acids in increasing lymphocytes. Indeed, unlike starvation during which leptin release is suppressed, infection leads to a rapid and robust leptin release from the fat, and furthermore, leptin has been shown to enhance the function of immune organs[46]. Here we obtained results suggesting that hypothalamus-induced fatty acid release might require the simultaneous leptin release to induce or optimize the effects on systemic lymphocytes. If so, a subsequent question is whether there are other secretory adipose factors in mediating the effects of hypothalamus-induced lipolysis on adaptive immunity. Clearly, future research is demanded to depict these molecules in the central regulation of adaptive immunity by the brain–fat axis.

Thus, the brain represents a critical player in conveying innate immunity signal TNF to adaptive immune response. As elucidated in the conceptual model (**Supplementary Fig. 8**), we demonstrated that the brain action of TNF is sufficient to initiate the increases of peripheral T and B cells, and this effect is mediated by hypothalamic TNF receptor pathway. This function of hypothalamic TNF in initiating adaptive immunity is mediated at least through hypothalamus-induced lipolysis. In conclusion, the hypothalamus–fat axis plays an important role in rapidly linking innate immune signal to adaptive immune responses.

Methods

Animals and peripheral treatments

Tnfrsf1a^{tm1Im}/*Tnfrsf1b*^{tm1Imx}/J mice and wild-type C57BL/6 mice were purchased from the Jackson Laboratory. *Pomc-Cre* mice were produced as previously described[47]. All mice were maintained on C57BL/6 stain background. Mice were housed in standard, pathogen-free conditions with 12 h/12 h light and darkness cycles and maintained on a normal chow diet, and male mice at adult ages (3–5 months) were used in experiments. C57BL/6 mice with diet-induced obesity were generated through 15-week high-fat diet feeding, and age-matched chowfed C57BL/6 mice were used as controls. For pharmacological injections, mice were intraperitoneally (i.p.) injected with TNF, palmitic acid, linoleic acid, cerulenin (Sigma), recombinant mouse leptin, and mouse leptin neutralizing antibody (R&D systems)

at the indicated doses consecutively for 3 d. For bacterial injection, mice were intravenously injected with *L. monocytogenes* (ATCC) at the dose of 5×10^4 CFU (colony-forming units). Mice were euthanized at indicated times post treatment, and various tissues were collected for subsequent analyses. The Institutional Animal Care and Use Committee at the Albert Einstein College of Medicine approved all the procedures.

Hypothalamic third ventricle cannulation and injections

Hypothalamic third ventricle cannulation was performed as previously described[8,9,11]; briefly, we employed an ultraprecise small animal stereotactic apparatus (Kopf Instruments) to implant a 26-gauge guide cannula (Plastics One) at the midline coordinates of 1.8 mm posterior to the bregma and 5.0 mm below the bregma. Mice were given 1 to 2 weeks for complete surgical recovery, and were injected via cannula with TNF (Sigma) or WP9QY (AnaSpec) at the indicated doses dissolved in 0.5 ul of artificial cerebrospinal fluid (aCSF) over a duration of 5 min. Injection of aCSF was used as the vehicle control. Intra-MBH injection which primarily targeted the arcuate nucleus was performed as previously described[11]. Briefly, injections were directed on an ultra-precise stereotactic apparatus at coordinates of 1.5 mm posterior to bregma, 5.8 mm below the surface of skull and 0.3 mm lateral to midline. Purified lentiviruses suspended in 0.2 ul aCSF were injected over 10-min period via a 26-gauge guide cannula and a 33-gauge internal injector connected to a 5-ul Hamilton Syringe and infusion pump (WPI Instruments).

Lentiviruses and histology

As described previously[11], we cloned TNFR1 cDNA (Sigma) into a synapsin promoter-driven lentiviral expression system, and cloned TNFR1 or TNFR2 shRNA (Sigma) into a lentiviral shRNA system. Lentiviruses were generated and amplified using HEK 293T cells and then purified as previously described[11]. Brain histology was analyzed using brain sections and immunostaining. Briefly, mice under anesthesia were transcardially perfused with 4% PFA and brains were removed, fixed, and post-fixed in 4% PFA, and infiltrated with 20–30% sucrose. Tissue sections were cut according to 20 um thickness, blocked, penetrated with 0.2% Triton-X 100, treated with rabbit anti-TNFR1 (polyclonal, Abcam, 1:1,000), mouse anti-TNFR2 (clone L-20, Santa Cuz, 1:1,000), or mouse anti-BrdU (clone Bu20a, Cell signaling, 1:1000) primary antibody, and subsequently reacted with a fluorescent secondary antibody (Invitrogen, 1:1,000). BrdU staining: mice were injected with BrdU (Invitrogen) at the dose of 30 mg per kg of body weight for 2 h before these animals were perfused. Naive IgG (clone DA1E, Cell signaling) of appropriate species were used as negative controls. DAPI staining was used to reveal all cells in the sections. Images were captured using confocal microscopy.

Epididymal fat denervation

Denervation of epididymal fat was performed as described previously[28]. In this procedure, mice were anesthetized, a small skin incision on the lower abdominal portion was made to invade the peritoneal cavity, and subsequently, the vascular strand innervating the epididymal fat pad was identified with laparotomy. The nerve bundle from the vessels was

carefully dissected and cut with a scissor, followed by a local application of phenol. The tissue was cleaned with sterile saline and skin was closed with sterile sutures.

Flow cytometry

Spleen was minced with DMEM, filtered through 100-μm cell strainer, and after centrifugation, then were incubated with Lysing Buffer (BD Pharm lyse) for cell isolation for 5 min at 25 °C, and isolated via centrifugation. Epididymal fat was carefully dissected, minced with scalpel, digested with Liberase TM research Grade (Roche) for 20 min at 37 °C, filtered through 100-μm cell strainer, and pelleted via centrifugation for cell suspension. Blood was collected and incubated with Lysing Buffer (BD Pharm lyse) for 5 min at 25 °C, and single cells were prepared through centrifugation. Single suspension cells from these tissues were washed twice, and cell yields and viability were assessed via trypan blue. 1×10^6 cells of single suspension cells were adjusted and blocked with CD16/CD31 (FcR Block, BD Pharmingen) at 4 °C for 10 min for flow cytometry. Single-suspension cells were reacted at 4 °C for 20 min with the antibodies including: anti-CD4 FITC (clone GK 1.5, eBioscience), anti-CD8 APC (clone 53-6.7, BD Pharmingen), anti-CD3 PE (clone 145-2c11, eBioscience), anti-B220 PE-Cy7 (clone RA3-6B2, Biolegend), anti-F4/80 APC (clone BM8, eBioscience), anti-CD11b FITC (clone M1/70, BD Pharmingen), anti-CD11c PE (clone HL3, BD Pharmingen), anti-CD278 (ICOS) FITC (clone 7E.17G9, eBioscience), anti-CD279 (PD-1) PE-Cy7 (clone J43, eBioscience), anti-CD274 (PD-L1) PE (clone MIH5, eBioscience), anti-CD183 (CXCR3) BV421 (clone CXCR3-173, BD Horizon), anti-CD196 (CCR6) Alexa 647 (clone 140706, BD Pharmingen). Intracellular staining for anti-Foxp3 Alexa Fluor488 (clone FJK-16s, eBioscience) was conducted using BD Cytofix/Cytoperm Plus (BD Pharmingen). Lymphocyte subpopulations reacted with fluorescence-activated cell sorter antibodies were measured on a LSR II flow cytometer (BD Bioscience) and the analyzed via FlowJo program (BD Bioscience).

Biochemical assays

Serum-free fatty acids were determined biochemically using acyl-CoA synthetase–acyl-CoA oxidase (ACS-ACOD) with NEFA-HR (Wako) according to the manufacturer's instruction. TNF concentrations in the serum and CSF of mice were determined using Mouse TNF ELISA kit (eBioscience) according to the manufacturer's instruction. Serum leptin concentrations were measured using Mouse Leptin ELISA Kit (Crystal Chem). CSF collection was performed as previously described[48]; briefly, an anesthetized mouse was fixed on the stereotactic apparatus with the head was placed to an angle of ~135° from the body, then a sagittal incision in the neck skin was applied to inferior to the occiput, followed by penetrating a capillary tube through the dura mater into the cisterna magna to draw the CSF. Metabolomics: ^{2}H-labeling of fatty acid was determined as described previously[49]. After labeling of ^{2}H, fatty acids were derivatized using diazomethane. Fatty acid methyl esters were formed by dissolving the extracted fatty acids in 50 μl of methanol and adding 300 μl of ether-diazomethane. The sample was allowed to react at 25 °C for 45 min. The fatty acid methyl esters were then dissolved in 100 μl of chloroform and analyzed by gas chromatography-electron impact ionization mass spectrometry. To account for possible differences in the ionization efficiency of each fatty acid, the profile was compared against standards prepared by mixing known quantities of each fatty acid.

Quantitative RT-PCR

Tissues were homogenized and extracted for RNA using TRIzol (Invitrogen). Complementary DNA was synthesized using M-MLV Reverse Transcriptase kit (Promega) and subjected to PCR amplification using SYBR Green PCR Master Mix (Applied Biosystems). PCR results were normalized against TATA box binding protein (*Tbp*) or *Actb* expression. Primer sequences are:

Lipe, 5′-TGTTGGGGTGACTCTAACGC-3′ and 5′-GTCTTCTGCGAGTGTCACCA-3′

Lpl, 5′- CCAGCTGGGCCTAACTTTGA-3′ and 5′-AACTCAGGCAGAGCCCTTTC-3′

Acsl1, 5′-GCCTCACTGCCCTTTTCTGA-3′ and 5′-GGCTGATGATTTCCACCCCA-3′

Nfkbia, 5′-TGAAGGACGAGGAGTACGAGC-3′ and 5′-TTCGTGGATGATTGCCAAGTG-3′

Il1b, 5′-GCTCAGGGTCACAAGAAACC-3′ and 5′-CATCAAAGCAATGTGCTGGT-3′

Il6, 5′-GAGATCGACTCTCTGTTCGAGG-3′ and 5′-GCCCGTTGAAGAAGTCCTG-3′

Socs3, 5′-ATGGTCACCCACAGCAAGTTT-3′ and 5′-TCCAGTAGAATCCGCTCTCCT-3′

Actb, 5′-CCAACTGGGACGACATGGAGA-3′ and 5′-CATGGCTGGGGTGTTGAAGG-3′

Tbp, 5′-ACCCTTCACCAATGACTCCTATG-3′ and 5′-TGACTGCAGCAAATCGCTTGG-3′

Statistical Analysis

ANOVA and Tukey's post-hoc test were used for comparisons involving more than two groups. Two-tailed Student's *t*-test was used for comparisons only involving two groups. Sample sizes were designed with adequate power according to the literature and our previous studies. Animals were randomly divided into experimental groups, and the investigators were not blind to group allocations. Data met normal distribution with similar variance between groups being compared. Data were presented as mean ± s.e.m. $P < 0.05$ was considered statistically significant.

Supplementary Material

Refer to Web version on PubMed Central for supplementary material.

ACKNOWLEDGEMENTS

The authors sincerely thank Cai's laboratory members for technical assistance. This study was supported by NIH R01 DK078750, R01 AG031774, R01 HL113180, and R01 DK 099136 (all to D. Cai).

Reference list

1. Beutler B. Innate immunity: an overview. Mol. Immunol. 2004; 40:845–859. [PubMed: 14698223]

2. Janeway CA Jr. Medzhitov R. Innate immune recognition. Annu. Rev. Immunol. 2002; 20:197–216. [PubMed: 11861602]
3. Rubartelli A, Lotze MT. Inside, outside, upside down: damage-associated molecular-pattern molecules (DAMPs) and redox. Trends. Immunol. 2007; 28:429–436. [PubMed: 17845865]
4. Hoebe K, Janssen E, Beutler B. The interface between innate and adaptive immunity. Nat. Immunol. 2004; 5:971–974. [PubMed: 15454919]
5. Kabelitz D, Medzhitov R. Innate immunity--cross-talk with adaptive immunity through pattern recognition receptors and cytokines. Curr. Opin. Immunol. 2007; 19:1–3. [PubMed: 17157490]
6. Banyer JL, Hamilton NH, Ramshaw IA, Ramsay AJ. Cytokine in innate and adaptive immunity. Rev. Immunogenet. 2000; 2:359–373. [PubMed: 11256745]
7. Purkayastha S, et al. Neural dysregulation of peripheral insulin action and blood pressure by brain endoplasmic reticulum stress. Proc. Natl. Acad. Sci. USA. 2011; 108:2939–2944. [PubMed: 21282643]
8. Purkayastha S, Zhang G, Cai D. Uncoupling the mechanisms of obesity and hypertension by targeting hypothalamic IKK-beta and NF-kappaB. Nat. Med. 2011; 17:883–887. [PubMed: 21642978]
9. Zhang G, et al. Hypothalamic programing of system ageing involving IKK-beta, NF-kappaB and GnRH. Nature. 2013; 497:211–216. [PubMed: 23636330]
10. Li J, Tang Y, Cai D. IKKbeta/NF-kappaB disrupts adult hypothalamic neural stem cells to mediate a neurodegenerative mechanism of dietary obesity and pre-diabetes. Nat. Cell Biol. 2012; 14:999–1012. [PubMed: 22940906]
11. Zhang X, et al. Hypothalamic IKKbeta/NF-kappaB and ER stress link overnutrition to energy imbalance and obesity. Cell. 2008; 135:61–73. [PubMed: 18854155]
12. Hamon M, Bierne H, Cossart P. Listeria monocytogenes: a multifaceted model. Nat. Rev. Microbiol. 2006; 4.:423–434. [PubMed: 16710323]
13. Pamer EG. Immune responses to Listeria monocytogenes. Nat. Rev. Immunol. 2004; 4:812–823. [PubMed: 15459672]
14. Gross PM. Circumventricular organ capillaries. Prog. Brain Res. 1992; 91:29–233. [PubMed: 1410412]
15. Mccusker RH, Kelly KW. Immune-neural connections: how the immune system's response to infectious agents influences behavior. J. Exp. Biol. 2013; 216:84–98. [PubMed: 23225871]
16. Meng Q, Cai D. Defective hypothalamic autophagy directs the central pathogenesis of obesity via the IkappaB kinase beta (IKKbeta)/NF-kappaB pathway. J. Biol. Chem. 2011; 286:32324–32332. [PubMed: 21784844]
17. Peschon JJ, et al. TNF receptor-deficient mice reveal divergent roles for p55 and p75 in several models of inflammation. J. Immunol. 1998; 160:943–952. [PubMed: 9551933]
18. Chen CP, Hertzberg M, Jiang Y, Graves DT. Interleukin-1 and tumor necrosis factor receptor signaling is not required for bacteria-induced osteoclastogenesis and bone loss but is essential for protecting the host from a mixed anaerobic infection. Am. J. Pathol. 1999; 155:2145–2152. [PubMed: 10595943]
19. Nguyen MT, et al. A subpopulation of macrophages infiltrates hypertrophic adipose tissue and is activated by free fatty acids via Toll-like receptors 2 and 4 and JNK-dependent pathways. J. Biol. Chem. 2007; 282:35279–35292. [PubMed: 17916553]
20. Saberi M, et al. Hematopoietic cell-specific deletion of toll-like receptor 4 ameliorates hepatic and adipose tissue insulin resistance in high-fat-fed mice. Cell Metab. 2009; 10:419–429. [PubMed: 19883619]
21. Shi H, et al. TLR4 links innate immunity and fatty acid-induced insulin resistance. J. Clin. Invest. 2006; 116:3015–3025. [PubMed: 17053832]
22. Konner AC, Bruning JC. Toll-like receptors: linking inflammation to metabolism. Trends Endocrinol. Metab. 2011; 22:16–23. [PubMed: 20888253]
23. Fessler MB, Rudel LL, Brown JM. Toll-like receptor signaling links dietary fatty acids to the metabolic syndrome. Curr. Opin. Lipidol. 2009; 20:379–385. [PubMed: 19625959]

24. Pearce EL, et al. Enhancing CD8 T-cell memory by modulating fatty acid metabolism. Nature. 2009; 460:103–107. [PubMed: 19494812]
25. Zu L, et al. Bacterial endotoxin stimulates adipose lipolysis via toll-like receptor 4 and extracellular signal-regulated kinase pathway. J. Biol. Chem. 2009; 284:5915–5926. [PubMed: 19122198]
26. Youngstrom TG, Bartness TJ. White adipose tissue sympathetic nervous system denervation increase fat pad cell number. Am. J. Physiol. 1998; 275:R1488–R1493. [PubMed: 9791065]
27. Cousin B, et al. Local sympathetic denervation of white adipose tissue in rats induces preadipocyte proliferation without noticeable changes in metabolism. Endocrinology. 1993; 133:2252–2262.
28. Buettner C, et al. Leptin controls adipose tissue lipogenesis via central, STAT3-independent mechanisms. Nat. Med. 2008; 14:667–675. [PubMed: 18516053]
29. Nishimura S, et al. CD8+ effector T cells contribute to macrophage recruitment and adipose tissue inflammation in obesity. Nat. Med. 2009; 15:914–920. [PubMed: 19633658]
30. Wu H, et al. T-cell accumulation and regulated on activation, normal T cell expressed and secreted upregulation in adipose tissue in obesity. Circulation. 2007; 115:1029–1038. [PubMed: 17296858]
31. Yang G, Parkhurst CN, Hayes S, Gan WB. Peripheral elevation of TNF-alpha leads to early synaptic abnormalities in the mouse somatosensory cortex in experimental autoimmune encephalomyelitis. Proc. Natl. Acad. Sci. USA. 2013; 110:10306–10311. [PubMed: 23733958]
32. Meisel C, et al. Central nervous system injury-induced immune deficiency syndrome. Nat. Rev. Neurosci. 2005; 6:775–786. [PubMed: 16163382]
33. Huston JM, et al. Splenectomy inactivates the cholinergic antiinflammatory pathway during lethal endotoxemia and polymicrobial sepsis. J. Exp. Med. 2006; 203:1623–1628. [PubMed: 16785311]
34. Sun J, Singh V, Kajino-Sakamoto R, Aballay A. Neuronal GPCR controls innate immunity by regulating noncanonical unfolded protein response genes. Science. 2011; 332:729–732. [PubMed: 21474712]
35. Rossa-Ballina M, et al. Splenic nerve is required for cholinergic antiiflammatory pathway control of TNF in endotoxemia. Proc. Natl. Acad. Sci. USA. 2008; 105:11008–11013. [PubMed: 18669662]
36. Pavlov VA, et al. Central muscarinic cholinergic regulation of the systemic inflammatory response during endotoxemia. Proc. Natl. Acad. Sci. USA. 2006; 103:5219–5223. [PubMed: 16549778]
37. Posey KA, et al. Hypothalamic proinflammatory lipid accumulation, inflammation, and insulin resistance in rats fed a high-fat diet. Am. J. Physiol. Endocrinol. Metab. 2009; 296:E1003–E1012. [PubMed: 19116375]
38. Thaler JP, et al. Obesity is associated with hypothalamic injury in rodents and humans. J. Clin. Invest. 2012; 122:153–162. [PubMed: 22201683]
39. Matarese G, et al. Hunger-promoting hypothalamic neurons modulate effector and regulatory T-cell response. Proc. Natl. Acad. Sci. USA. 2013; 110:6193–6198. [PubMed: 23530205]
40. Feuerer M, et al. Lean, but not obese, fat is enriched for a unique population of regulatory T cells that affect metabolic parameters. Nat. Med. 2009; 15:930–939. [PubMed: 19633656]
41. Winner B, Kohl Z, Gage FH. Neurodegenerative disease and adult neurogenesis. Eur. J. Neurosci. 2011; 33:1139–1151. [PubMed: 21395858]
42. Berg AH, Scherer PE. Adipose tissue, inflammation, and cardiovascular disease. Circ. Res. 2005; 96:939–949. [PubMed: 15890981]
43. Hotamisligil GS. Inflammation and metabolic disorders. Nature. 2006; 444:860–867. [PubMed: 17167474]
44. Sennello JA, et al. Regulation of T cell-mediated hepatic inflammation by adiponectin and leptin. Endocrinology. 2005; 146:2157–2164. [PubMed: 15677756]
45. Stenz FB, Kitabchi AE. Palmitic acid-induced activation of human T-lymphocytes and aortic endothelial cells with production of insulin receptors, reactive oxygen species, cytokines, and lipid peroxidation. Biochem. Biophys. Res. Commun. 2006; 346:721–726. [PubMed: 16782068]
46. Trotter-Mayo RN, Roberts MR. Leptin acts in the periphery to protect thymocytes from glucocorticoid-mediated apoptosis in the absence of weight loss. Endocrinology. 2008; 149:5209–5218. [PubMed: 18583419]

47. Xu AW, et al. PI3K integrates the action of insulin and leptin on hypothalamic neurons. J. Clin. Invest. 2005; 115:951–958. [PubMed: 15761497]

48. Yan J, et al. Obesity-and aging-induced excess of central transforming growth factor-beta potentiates diabetic development via an RNA stress response. Nat. Med. 2014; 20:1001–1008. [PubMed: 25086906]

49. Brunengraber DZ, et al. Influence of diet on the modeling of adipose tissue triglycerides during growth. Am. J. Physiol. Endocrinol. Metab. 2003; 285:E917–E925. [PubMed: 12799315]

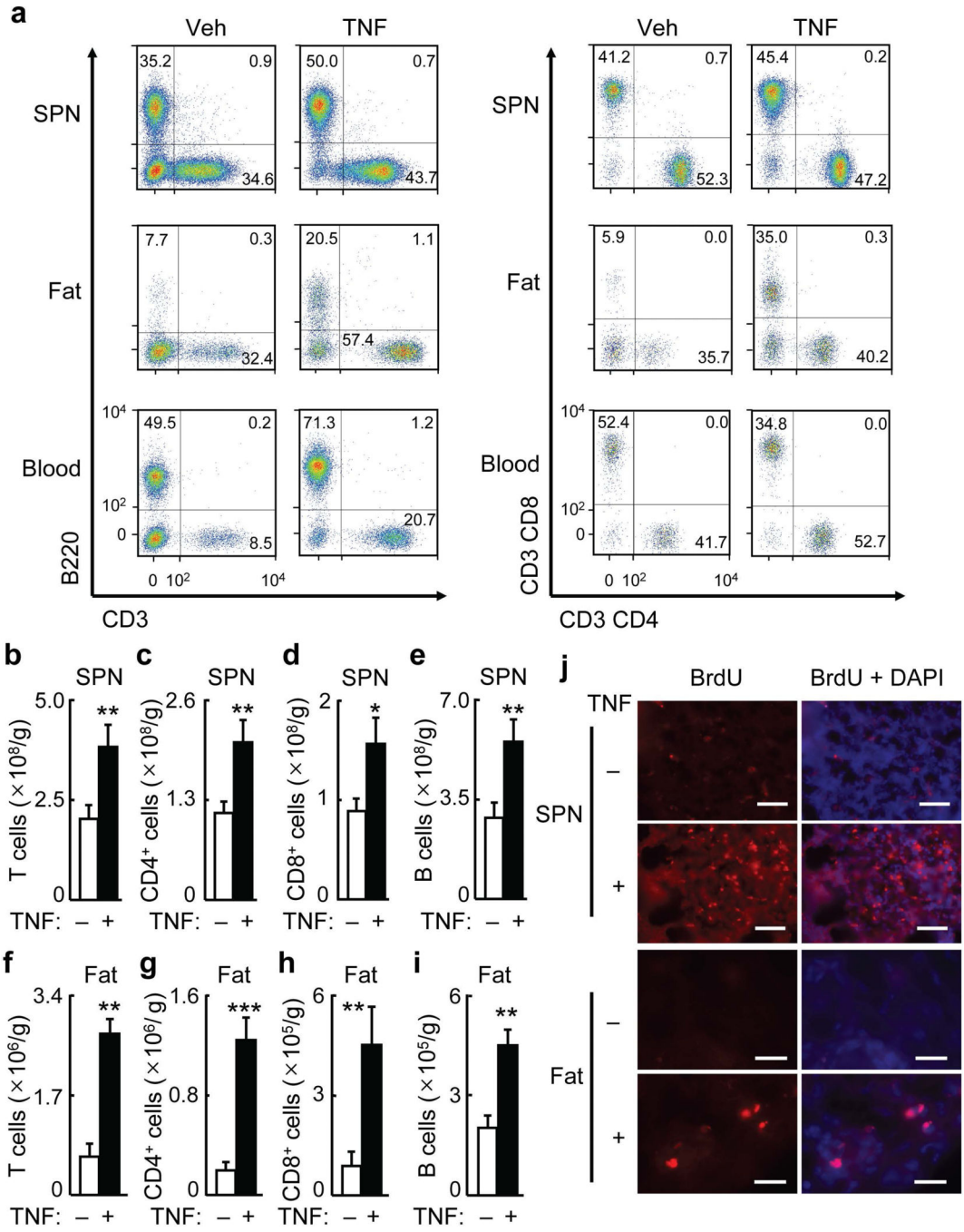

Figure 1.

Central TNF injection rapidly increases splenic and adipose lymphocytes.

C57BL/6 mice received daily TNF (10 pg) (+) vs. vehicle (Veh, −) injection in hypothalamic third ventricle for 3 days, and tissues were harvested for flow cytometry **(a–i)**, while some mice received i.p. BrdU injection at 2 hours prior to collection of tissues for BrdU staining **(j)**.

(a) Dot plots of T cells ($CD3^+$), B cells ($B220^+$), $CD4^+$ cells ($CD3^+CD4^+$), and $CD8^+$ cells ($CD3^+CD8^+$) in the spleen (SPN) (upper panels), epididymal fat (middle panels), and blood (lower panels). Dot plots represent 8–11 mice per group.
(b–e) Numbers of T cells ($CD3^+$) **(b)**, $CD4^+$ cells ($CD3^+CD4^+$) **(c)**, $CD8^+$ cells ($CD3^+CD8^+$) **(d)**, B cells ($B220^+$) **(e)** cells per gram of SPN.
(f–I) Numbers of T cells ($CD3^+$) **(f)**, $CD4^+$ cells ($CD3^+CD4^+$) **(g)**, $CD8^+$ cells ($CD3^+CD8^+$) **(h)**, B cells ($B220^+$) **(i)** cells per gram of epididymal fat.
(j) BrdU staining (red) of spleen and epididymal fat sections. DAPI staining (blue) was used to reveal all cells in tissue sections. Images represent 3–4 mice per group. Scale bar = 50 μm. $*P < 0.05$, $**P < 0.01$, $***P < 0.001$ (two-tailed Student's t-test); n = 8–11 mice per group (**b–i**). All data (mean) represent at least three independent experiments with similar observations (error bars, s.e.m.).

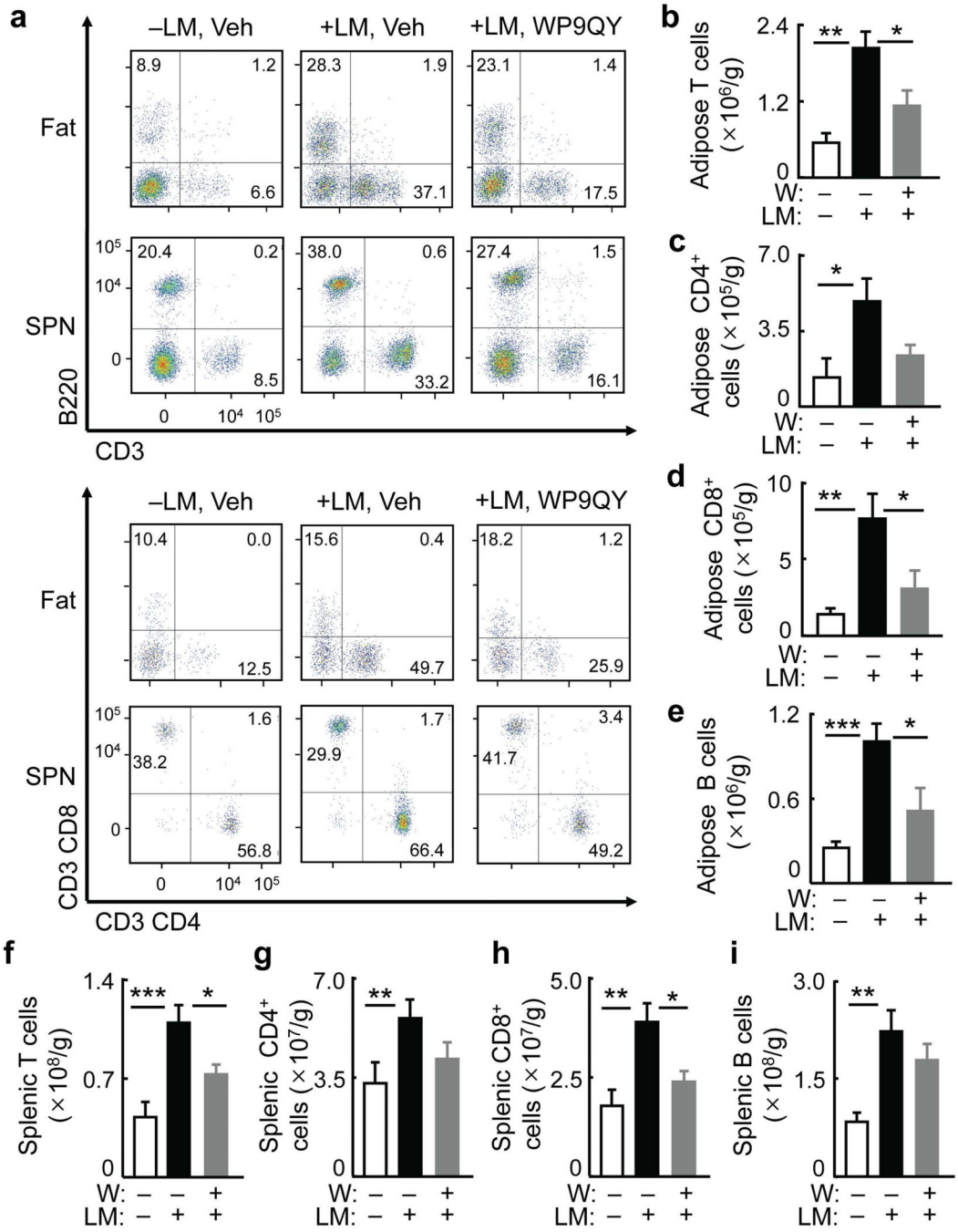

Figure 2.

Bacterial infection-induced adaptive immune response requires brain TNF.

C57BL/6 mice given pre-injection of the TNF antagonist WP9QY (W) or the vehicle artificial cerebrospinal fluid (Veh) into the hypothalamic ventricle 1 d before infection with *L. monocytogenes* (+LM) or vehicle (−LM) and then maintained with daily hypothalamic injection of WP9QY or vehicle for 3 d. After 3-day bacterial infection, mice were sacrificed and tissues were harvested for flow cytometry analysis.

(a) Dot plots of T cells ($CD3^+$), $CD4^+$ cells ($CD3^+CD4^+$), $CD8^+$ cells ($CD3^+CD8^+$) and B cells ($B220^+$) in the epididymal fat and spleen (SPN). Dot plots represent 6–8 mice per group.
(b–e) Numbers of T cells ($CD3^+$) **(b)**, $CD4^+$ cells ($CD3^+CD4^+$) **(c)**, $CD8^+$ cells ($CD3^+CD8^+$) **(d)** and B cells ($B220^+$) **(e)** per gram of epididymal fat.
(f–i) Numbers of T cells ($CD3^+$) **(f)**, $CD4^+$ cells ($CD3^+CD4^+$) **(g)**, $CD8^+$ cells ($CD3^+CD8^+$) **(h)** and B cells ($B220^+$) **(i)** per gram of spleen.
$^*P < 0.05$, $^{**}P < 0.01$, $^{***}P < 0.001$ (ANOVA, Tukey's post-hoc); n = 6–8 mice per group (**b– i**). All data (mean) represent two independent experiments with similar observations (error bars, s.e.m.).

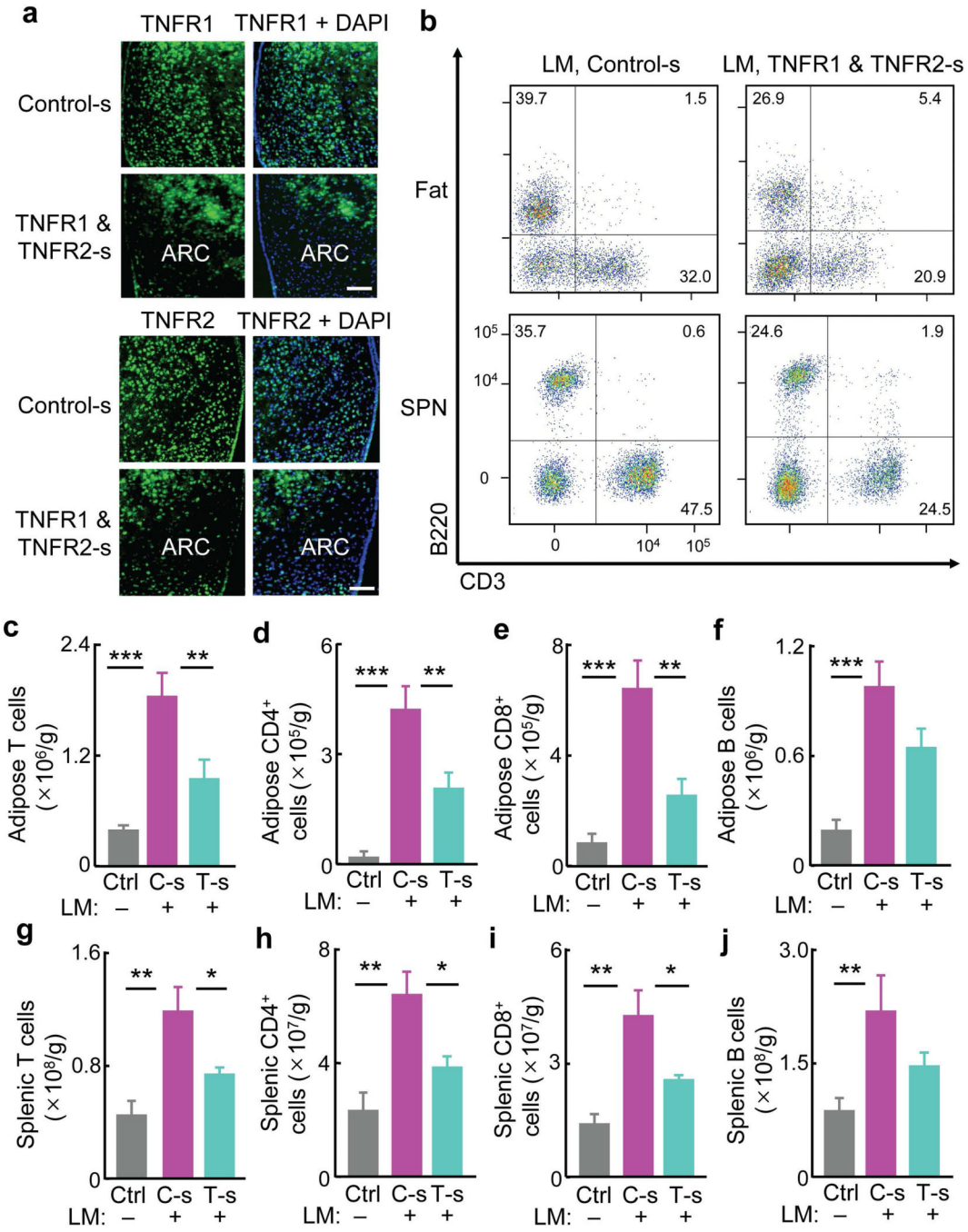

Figure 3.

Hypothalamic TNF receptor is required for adaptive immune response in infection. Standard C57BL/6 mice were bilaterally injected in the arcuate nucleus (ARC) with lentiviral TNFR1 and TNFR2 shRNA (TNFR1 & TNFR2-s, T-s) vs. nontargeting control shRNA (Control-s, C-s), and after 1-week recovery, these mice were infected with *Listeria monocytogenes* (LM, +) vs. vehicle (−) via intravenous injection. Control mice that did not receive LM injection were included as basal controls (Ctrl). After 3-day bacterial infection, mice were sacrificed and tissues were harvested for flow cytometry analysis.

(a) TNFR1 or TNFR2 immunostaining (green) of the MBH. DAPI staining (blue) was used to reveal all cells in tissue sections. Images represent 3–4 mice per group. Scale bar = 200 μm.

(b) Dot plots of T cells ($CD3^+$) and B cells ($B220^+$) in epididymal fat and spleen (SPN). Dot plots represent 5–7 mice per group.

(c–j) Numbers of T cells ($CD3^+$) **(c,g)**, $CD4^+$ cells ($CD3^+CD4^+$) **(d,h)**, $CD8^+$ cells ($CD3^+CD8^+$) **(e,i)** and B cells ($B220^+$) **(f,j)** per gram of epididymal fat **(c–f)** or SPN **(g–j)**. $*P < 0.05$, $**P < 0.01$ (ANOVA, Tukey's post-hoc); n = 5–7 mice per group (**c–j**). All data (mean) represent two independent experiments with similar observations (error bars, s.e.m.).

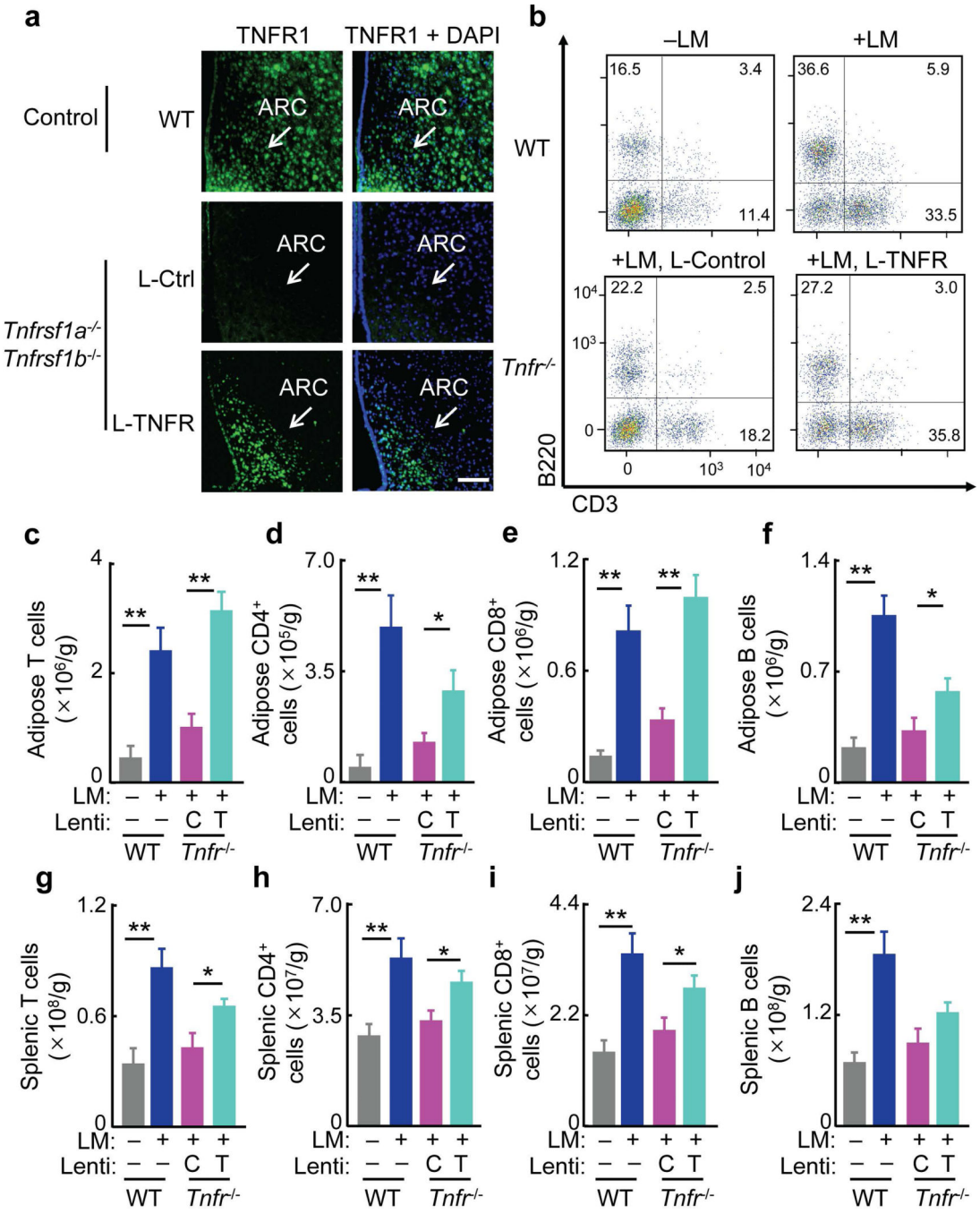

Figure 4.

Hypothalamic TNFR restoration improves adaptive immunity in TNFR-null mice. TNFR-null mice (*Tnfrsf1a*$^{-/-}$ *Tnfrsf1b*$^{-/-}$, *Tnfr*$^{-/-}$) and wild-type (WT) mice were bilaterally injected in the arcuate nucleus (ARC) with lentiviral TNFR1 (L-TNFR, T) vs. lentiviral control (L-Ctrl, C), and after 1-week recovery, these mice were infected with *Listeria monocytogenes* (+LM or +) via intravenous injection. WT mice without receiving LM injection (–LM or –) were included to provide the basal profiles. After 3-day bacterial infection, mice were sacrificed and tissues were harvested for flow cytometry analysis.

(a) TNFR1 immunostaining (green) of the MBH. DAPI staining (blue) was used to reveal all cells in tissue sections. Images represent 3–4 mice per group. Scale bar = 200 μm.
(b) Dot plots of T cells ($CD3^+$) and B cells ($B220^+$) in epididymal fat. Dot plots represent 5–7 mice per group.
(c–j) Numbers of T cells ($CD3^+$) **(c,g)**, $CD4^+$ cells ($CD3^+CD4^+$) **(d,h)**, $CD8^+$ cells ($CD3^+CD8^+$) **(e,i)** and B cells ($B220^+$) **(f,j)** per gram of epididymal fat **(c–f)** and spleen **(g–j)**.
$^*P < 0.05$, $^{**}P < 0.01$ (ANOVA, Tukey's post-hoc); n = 5–7 mice per group (**c–j**). All data (mean) represent two independent experiments with similar observations (error bars, s.e.m.).

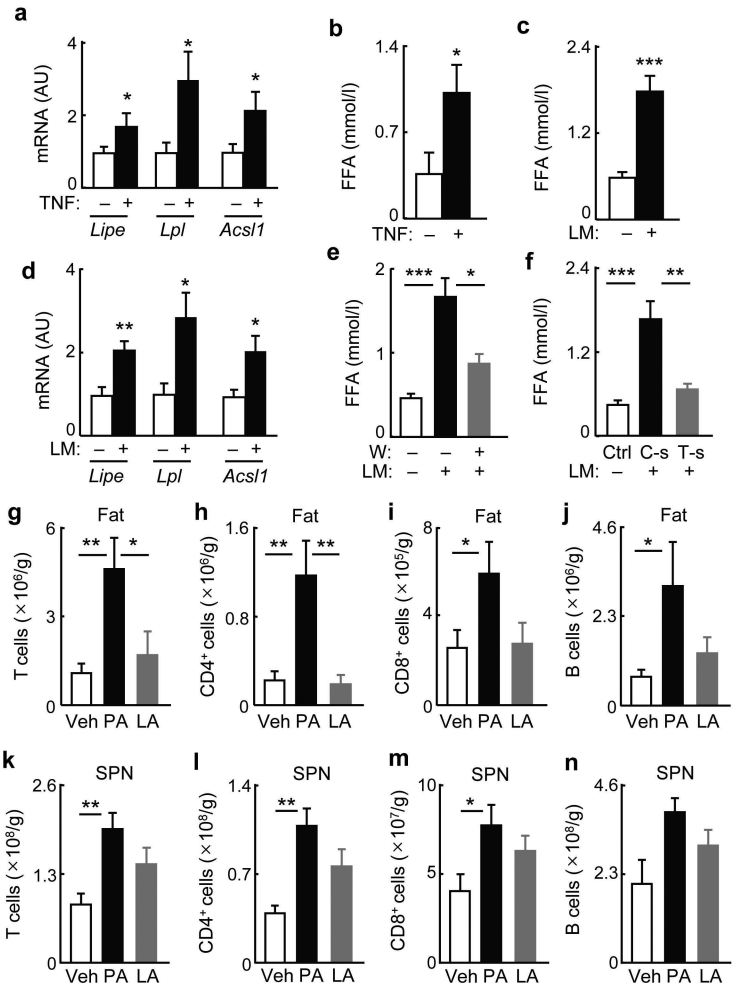

Figure 5.

Central induction of lipolysis mediates initiation of adaptive immune response.

(a–f) C57BL/6 mice received TNF (10 pg) (+) vs. vehicle (−) injection in hypothalamic third ventricle **(a,b)** as described in Fig. 1, or were injected with *Listeria monocytogenes* (LM, +) vs. vehicle (−) **(c,d)**, co-treated with TNF antagonist WP9QY (W) and LM injection **(e)** as described in Fig. 2, or treated with lentiviral TNFR1 & TNFR2 shRNA (T-s) vs. lentiviral scramble shRNA (C-s) (**f**) as described in Fig. 3, and following these treatments at the same time points as described in Fig. 1 to 3, epididymal fat and blood were harvested for measuring adipose mRNA levels of indicated genes **(a, d)** and serum FFA levels **(b,c,e,f)**. **(g–j)** C57BL/6 mice received daily i.p. injections of palmitic acid (PA), lenoleic acid (LA) vs. vehicle (Veh) for 3 days, and tissues were then harvested for flow cytometry analysis. Data show numbers of T cells ($CD3^+$) **(g,k)**, $CD4^+$ cells ($CD3^+CD4^+$) **(h,l)**, $CD8^+$ cells ($CD3^+CD8^+$) **(i,m)** and B cells ($B220^+$) **(j,n)** per gram of epididymal fat **(g–j)** or spleen (SPN) **(k–n)**.

P* < 0.05, ***P* < 0.01 (ANOVA, Tukey's post-hoc); n = 4–6 mice per group (a–f**), n = 5–6 mice per group (**g–n**). All data (mean) represent at least three independent experiments with similar observations (error bars, s.e.m.).

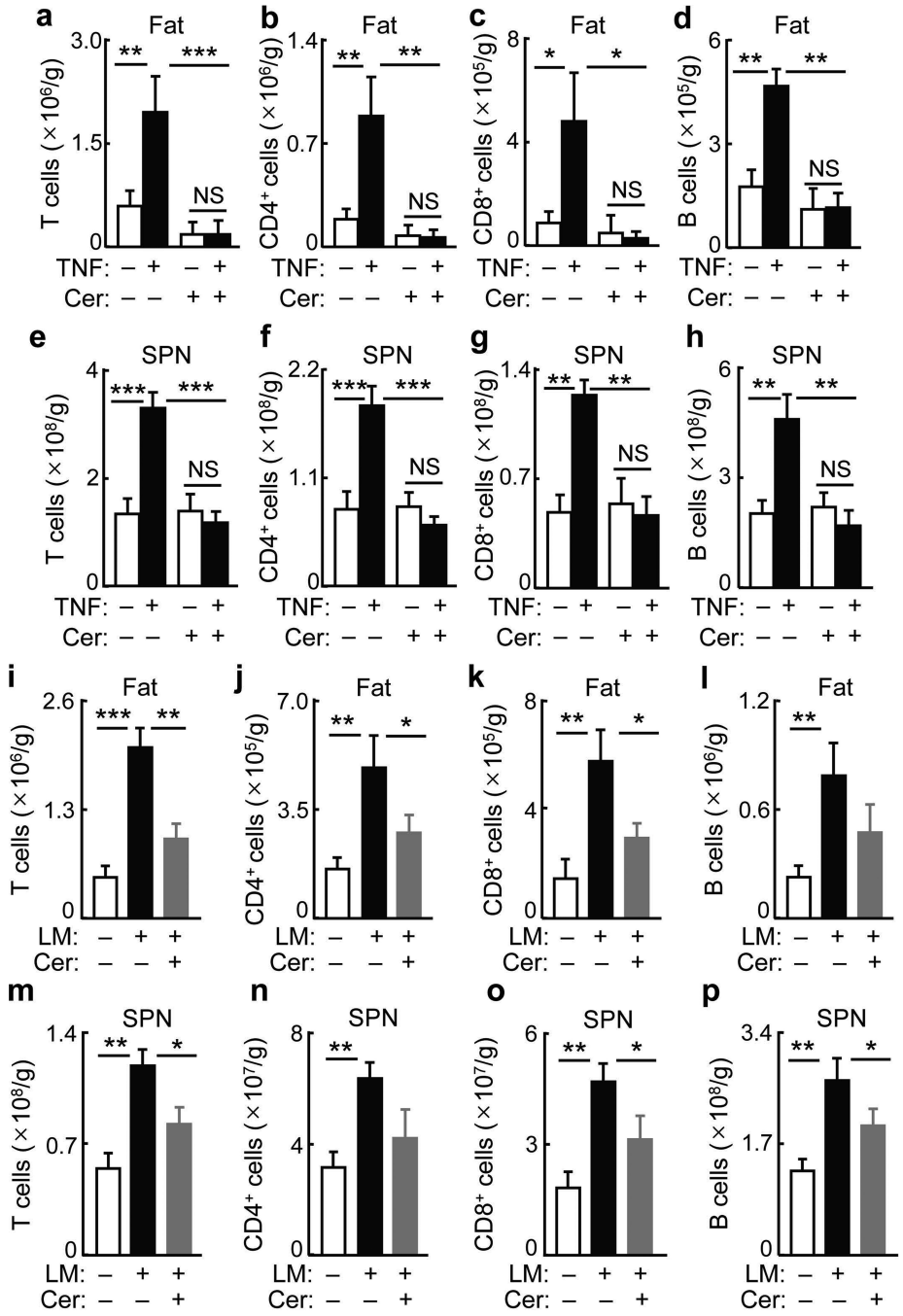

Figure 6.

Fatty acid inhibition attenuates brain TNF- or infection-induced adaptive immunity. Standard C57BL/6 mice received an i.p. injection of cerulenin (Cer, $_{+}$) vs. vehicle saline (−) on the day prior to other treatments **(a–p)**, followed by daily hypothalamic third-ventricle injections of 10 pg TNF (+) vs. vehicle aCSF (−) together with daily i.p. injections of cerulenin for 3 days (**a–h**), or followed by a single intravenous injection of *Listeria monocytogenes* (LM, +) vs. the vehicle (−) while daily i.p. injections of cerulenin continued for 3 days **(i–p)**. Following these treatments, tissues were harvested and subjected to flow

cytometry analysis. Data show numbers of T cells ($CD3^+$) **(a,e,i,m)**, $CD4^+$ cells ($CD3^+$ $CD4^+$) **(b,f,j,n)**, $CD8^+$ cells ($CD3^+$ $CD8^+$) **(c,g,k,o)** and B cells ($B220^+$) **(d,h,l,p)** per gram of epididymal fat **(a–d,i–l)** or spleen (SPN) **(e–h,m–p)** in TNF-injected **(a–h)** or LM-infected mice **(i–p)**.

$^*P < 0.05$, $^{**}P < 0.01$, $^{***}P < 0.001$ (ANOVA, Tukey's post-hoc); n = 5–7 mice per group. All data (mean) represent at least three independent experiments with similar observations (error bars, s.e.m.).

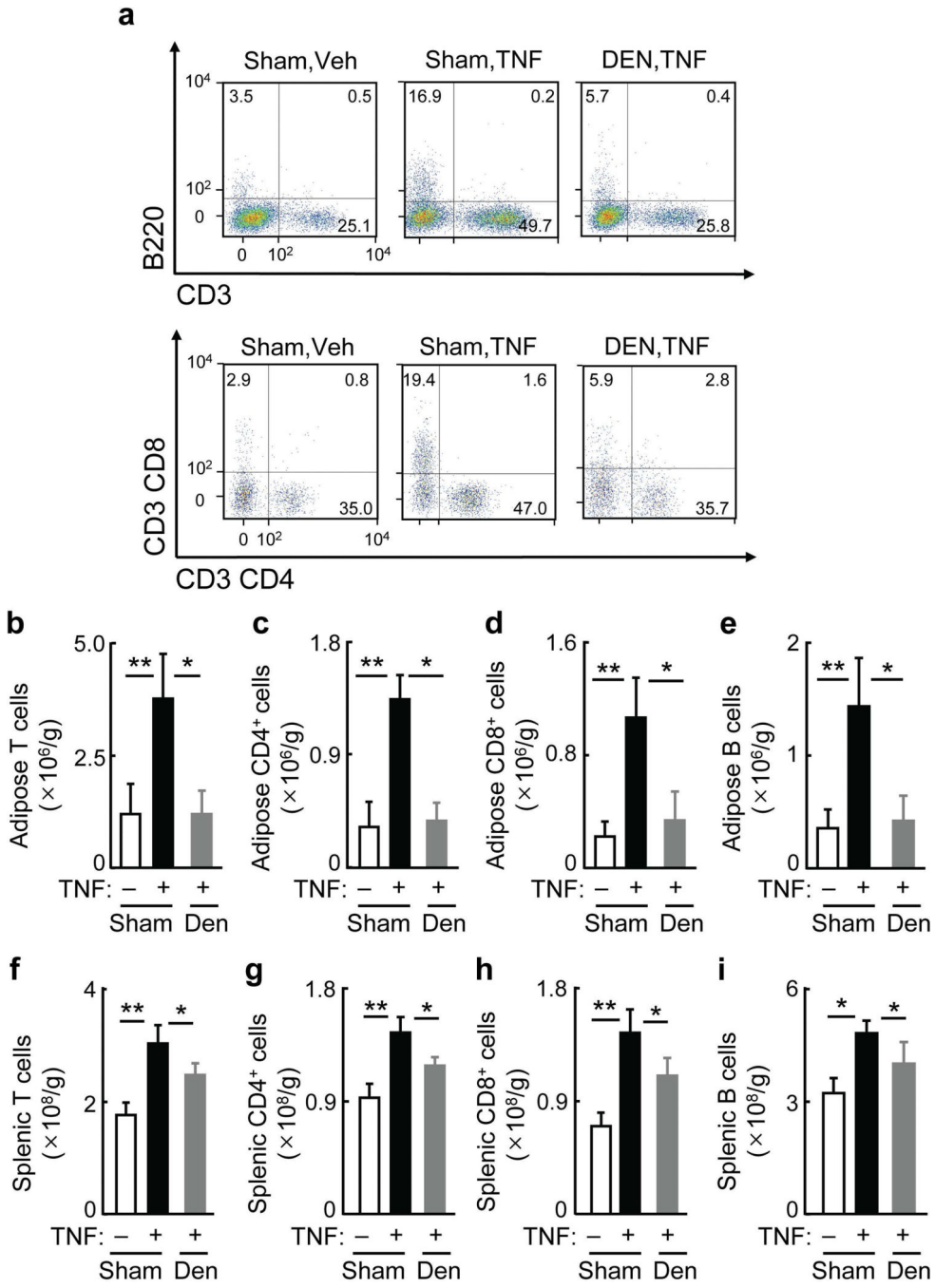

Figure 7.

Acute effect of the brain–fat axis on adaptive immunity is mediated by adipose nerve. C57BL/6 mice received epididymal fat denervation (Den) vs. sham surgery and at the same time were implanted with cannula in hypothalamic third ventricle, and following 1-week recovery, these animals received 3-day daily injections of TNF (10 pg) (+) vs. vehicle (−) via the pre-implanted cannula for 3 days, and tissues were harvested for flow cytometry. **(a)** Dot plots of T cells ($CD3^+$), B cells ($B220^+$), $CD4^+$ cells ($CD3^+$ $CD4^+$) and $CD8^+$ cells ($CD3^+$ $CD8^+$) in epididymal fat. Dot plots represent 7–8 mice per group.

(b–i) Numbers of T cells ($CD3^+$) **(b,f)**, $CD4^+$ cells ($CD3^+$ $CD4^+$) **(c,g)**, $CD8^+$ cells ($CD3^+$ $CD8^+$) **(d,h)** and B cells ($B220^+$) **(e,i)** per gram of epididymal fat **(b–e)** and spleen **(f–i)**. $*P < 0.05$, $**P < 0.01$ (ANOVA, Tukey's post-hoc); n = 7–8 mice per group (**b–j**). All data (mean) represent three independent experiments with similar observations (error bars, s.e.m.).

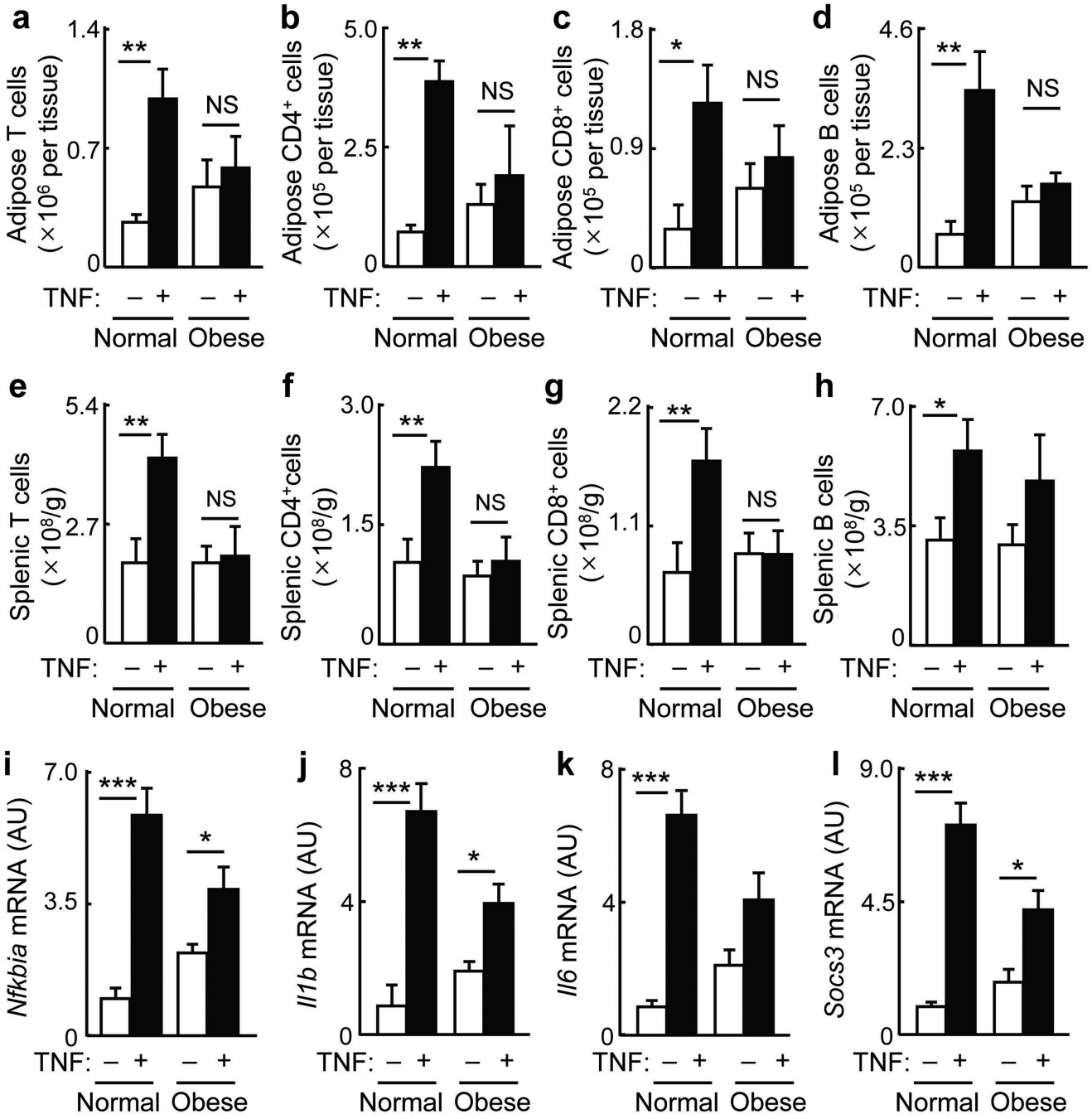

Figure 8.

Chronic neuroinflammation desensitizes the central regulation of adaptive immunity. Adult C57BL/6 mice received HFD feeding to develop obesity, and matched mice maintained on a normal chow were used as normal controls. These mice received daily injections of TNF (+) vs. vehicle (−) in the hypothalamic third ventricle for 3 days, and tissues were harvested for flow cytometry **(a–h)** and inflammatory gene expression in the hypothalamus **(i–l)**. Data in **(a–h)** show numbers of T cells ($CD3^+$) **(a,e)**, $CD4^+$ cells ($CD3^+$ $CD4^+$) **(b,f)**, $CD8^+$ cells

(CD3$^+$ CD8$^+$) **(c,g)** and B cells (B220$^+$) **(d,h)** per epididymal fat (**a–d**) or per gram of spleen (**e–h**).

*P < 0.05, **P < 0.01, ***P < 0.001(ANOVA, Tukey's post-hoc); All data (mean) represent two independent experiments with similar observations (error bars, s.e.m.).